JOURNAL OF MATERIALS SCIENCE 31 (1996) 4793–4799

Anisotropic photoluminescence characteristics of $Al_{0.08}Ga_{0.92}As$ single quantum well laser structure

P. S. DOBAL, H. D. BIST
Department of Physics and Center for Laser Technology, Indian Institute of Technology, Kanpur 200 016, India

G. MORELL, A. REYNES-FIGUERORA, A. MANIVANNAN, R. S. KATIYAR
University of Puerto Rico, Box 23343, San Juan, PR 00931, USA

S. K. MEHTA, R. K. JAIN
Solid State Physics Laboratory, Delhi, India

A nominal well width (20 nm) of $Al_{0.08}Ga_{0.92}As$ quantum well structure has been fabricated by molecular beam epitaxy technique with the aim of obtaining a lasing device. The temperature evolution of quantum well photoluminescence was studied in the range 10–300 K which shows excitons being trapped at the interfacial defects below 100 K. The linear polarization effects in the photoluminescence have been studied for the incident and collected light propagating parallel to the plane of the well layer. In a very careful study, the luminescence was found to be fully polarized for the incident electric vector parallel to well layers, while it showed depolarized behaviour for the incident electric vector perpendicular to the well layers. The earlier conclusions based on photoluminescence excitation and absorption studies of heavy- and light-hole emissions are supported. The 20 nm quantum well structure has been corroborated using scanning tunnelling microscopy.

1. Introduction

Two-dimensional confinement greatly enhances excitonic effects in quantum well (QW) structures. Room temperature excitonic resonances [1] in such structures have been used for high speed modulators [2], optical switches [3], mode locking of diode lasers [4], etc. For the reduced dimensionality of quantum wells (QWs), one also expects anisotropic band-to-band transitions for light propagating parallel to the plane of the layers. This explains the polarization-dependent gain exhibited in the emission spectra by quantum well (QW) lasers [5]. The polarization dependence of spontaneous emission and optical gain coefficients can be explained qualitatively [6] in terms of the polarization-dependent transition moments [7] associated with light-hole and heavy-hole bands in QWs. The anisotropic absorption and emission processes, therefore, have a considerable effect on QW lasers. Anisotropic absorption for light-holes and heavy-holes has been observed in a single QW for light propagating along the well plane [8]. Photoluminescence excitation (PLE) spectroscopy is the most commonly employed technique to study the heavy- and light-hole emissions in semiconductor QWs [9]. In the present work, the polarization dependence of heavy-hole and light-hole recombinations is studied after deconvolution of the structures in the photoluminescence (PL). Experimental details are described in Section 2. The cross-sectional scanning tunnelling microscopy (STM) results are given in Section 3.1. A detailed analysis of PL and its dependence on excitation power, temperature, and polarization is given in Section 3.2.

2. Experimental details

Single quantum well (SQW) laser structures were fabricated by employing a Riber 2300 R&D molecular beam epitaxy (MBE) apparatus. A typical laser structure is shown in Fig. 1. On a 500 μm thick (1 0 0) GaAs substrate (*a*), a 1 μm thick GaAs buffer (*b*), 2 μm n-$Al_{0.7}Ga_{0.3}As$ cladding layer (*c*), 80 nm n-$Al_{0.3}Ga_{0.7}As$ barrier layer (*d*), 20 nm, $Al_{0.08}Ga_{0.92}As$ quantum well (*e*), followed by 80 nm p-$Al_{0.3}Ga_{0.7}As$ barrier layer (*f*), and 2 μm p-$Al_{0.7}Ga_{0.3}As$ cladding layer (*g*) capped by a 1 μm GaAs layer (*h*) were deposited in that order.

For PL measurements, the sample was mounted in a variable temperature cryostat. The incident excitation beam (514.5 nm) with its electric vector parallel to the SQW, was tightly focused with a cylindrical lens to produce a line focus (width $\leqslant$ 1 μm) along the well length. The focused beam covered all the QW length, though the width was still larger than the well width.

0022–2461

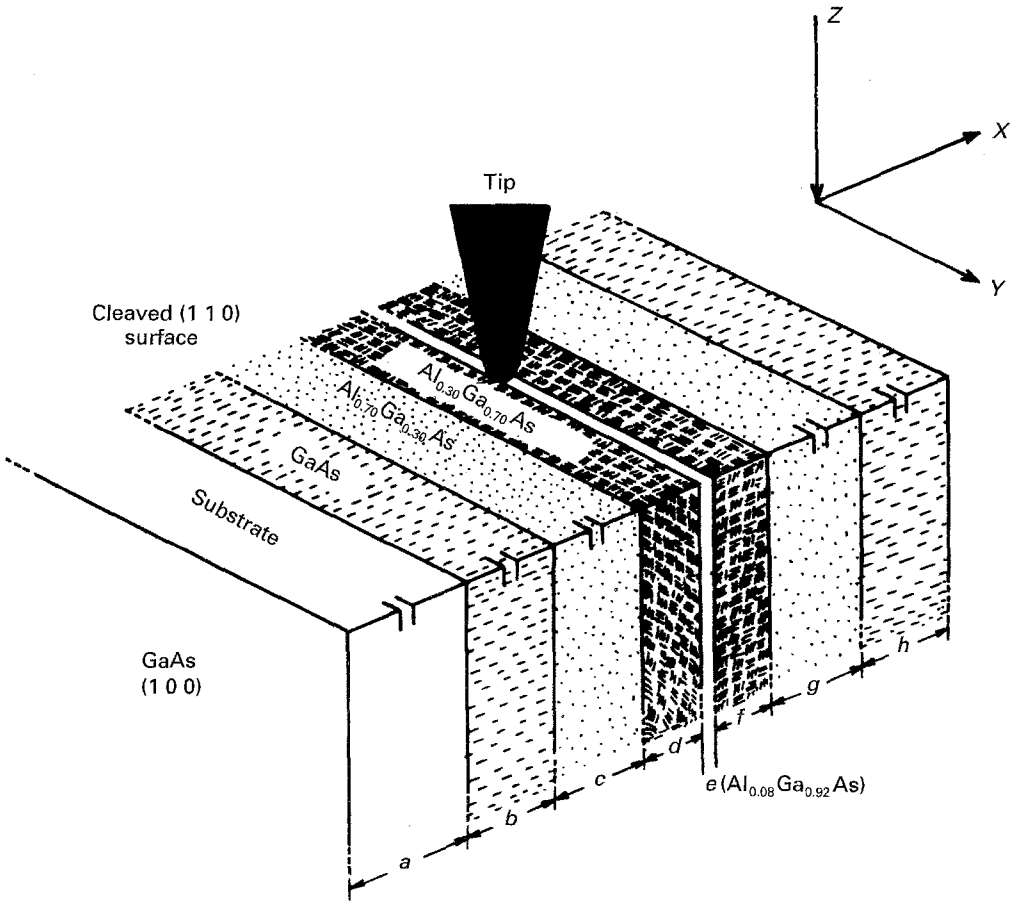

Figure 1 Schematic diagram of the $Al_{0.08}Ga_{0.92}As$ single quantum well laser structure and STM tip configuration. The GaAs, $Al_{0.3}Ga_{0.7}As$, and $Al_{0.7}Ga_{0.3}As$ layers are marked for their identification. Typical widths are $a = 500$ μm, $b = h = 1$ μm, $c = g = 2$ μm, $d = f = 80$ nm and $e = 20$ nm.

A polarization rotator was used to make the incident electric vector either parallel or perpendicular to the well layers. In both cases, the parallel and perpendicularly polarized components of the PL spectra at various points along the well width, were measured using a linear polarizer. The PL spectra have also been studied using the 638 nm line from a DCM Dye pumped by an Ar^+ laser. The temperature of the sample was varied in the range 10–300 K. The emission was dispersed utilizing a SPEX triplemate and detected by a cooled GaAs photomultiplier. All the data have been corrected for the response function of the photomultiplier and for the polarization bias of the spectrometer.

A nanoscope-III (Digital Instruments, Santa Barbara, CA, USA) was used to facilitate the scanning of the cross-sectional surface of the sample. The STM scanning tunnelling microscopy (STM) measurements were made in air utilizing cut Pt–Ir tips. The STM unit was placed on a tripod stand to isolate it from external vibrations. The piezoelectric scanner was calibrated using a high-grade graphite sample (ZYA, Union Carbide) prior to STM measurements.

3. Results and discussion

3.1. Scanning tunnelling microscopy

Scanning tunnelling microscopy (STM) is an extremely surface sensitive technique. It provides chemical and electronic information in the depth and in the lateral dimensions with atomic scale resolution [10]. Hence, there is growing interest in the analysis of epitaxially grown heterostructures utilizing the cross-sectional STM (XSTM) technique [11, 12]. In the present work, the samples were cleaved at room temperature and mounted vertically on copper plates to expose the (1 1 0) face of the layered structure directly to the tip of the STM. The XSTM image of the $Al_{0.08}Ga_{0.92}As$ SQW is shown in Fig. 2. The image was recorded in a constant height mode, with a sample voltage of 3.678 V and a tunnelling current of 222.3 pA. The observed contrast within the heterostructure layers is purely an electronic effect, since the cleavage face is automatically flat. The central white region is the $Al_{0.08}Ga_{0.92}As$ quantum well (20 nm) and the adjacent light dark and dark regions are the barrier layers of $Al_{0.3}Ga_{0.7}As$ and, the cladding layers of $Al_{0.7}Ga_{0.3}As$, respectively. The distinction between the outer layers in STM images was difficult to observe in the present case due to possible oxidation that might have occurred due to performing the cleavage in air. Within a given layer, significant fluctuation can be seen in the STM image. We attribute these fluctuations mainly to the dopant atoms within the layers.

3.2. Photoluminescence

3.2.1. Excitation power dependence

A simple way to analyse the origin of PL emission from semiconductor structure is to study its evolution

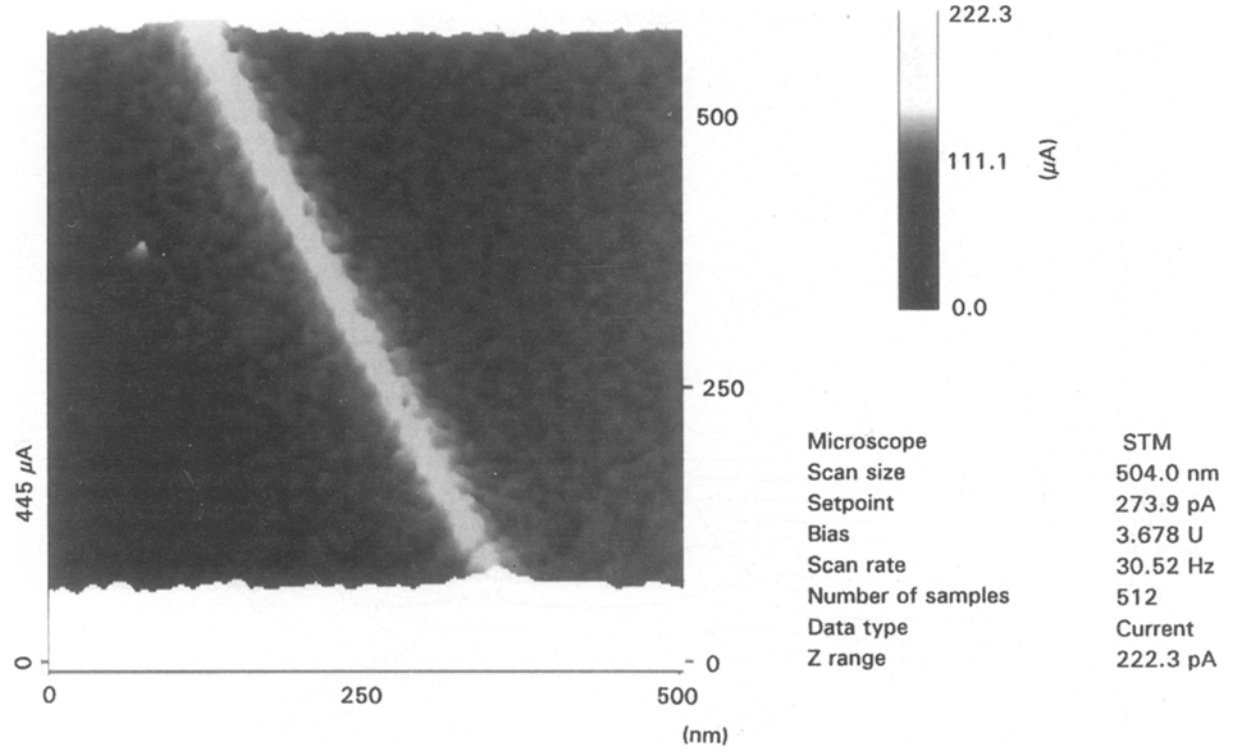

Figure 2 Large scale cross-sectional STM image of $Al_{0.08}Ga_{0.92}As$ single quantum well (SQW) laser structure. The STM bias voltage and demand current were 3.67 V and 222.3 pA, respectively.

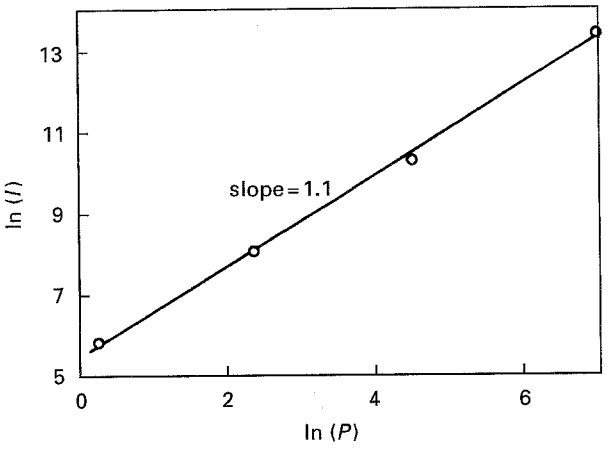

Figure 3 The logarithmic luminescence intensity [ln (*I*)] of quantum well emission at 10 K monitored at 1.592 eV as a function of excitation power [ln (*P*)].

with excitation power. Following the model of Fouquet and Seigman [13], we have measured the integrated intensity of the QW luminescence peak (1.592 eV at 10 K) in a range of three orders of magnitude of the excitation power (*P*). Fig. 3 depicts the natural logarithmic plot of intensity against the natural log of excitation power (*P*). A single valued slope (1.1) suggests purely excitonic recombination in the quantum well. These observations are in line with earlier results obtained from excitonic absorption [14] and time resolved PL experiments [15] in GaAs/AlGaAs multi quantum well structures (MQWSs) with well width ranging from 5 to 15 nm.

3.2.2. Temperature dependence

The PL spectra of $Al_{0.08}Ga_{0.92}As$ SQW at various temperatures, are shown in Fig. 4 by a 3-D diagram. In this case, the well was excited by the 638 nm line normal to the layers after etching away the top GaAs layer. At 10 K, a sharp structure in the PL spectrum is observed at 1.592 eV followed by a weaker line at 1.76 eV. These two peaks have been attributed to the recombinations in $Al_{0.08}Ga_{0.92}As$ QW and the barrier layers of $Al_{0.3}Ga_{0.7}As$, respectively. In Fig. 5, the variation of the PL peak energies with temperature is shown, in the range 10–300 K. The data points (○) and (+) represent the recombinations associated with $Al_{0.3}Ga_{0.7}As$ and $Al_{0.08}Ga_{0.92}As$ QW. For comparison, the temperature dependent band gap variation of bulk GaAs is plotted as curve (c) using the well known Varshni's relation. This curve has been suitably displaced from our experimental points. The $Al_{0.3}Ga_{0.7}As$ recombinations closely follow the bulk GaAs curve in the whole temperature range [curve (a)]. The QW PL peak [curve (b)] follows the bulk GaAs curve down to 100 K. Below this temperature it deviates from the GaAs plot remaining nearly constant in the 10–100 K range. In this range, the observed Stokes shift is between 3–6 meV. This shift is much smaller than the expected quantum well exciton binding energies [16]. Thus, in the range 10–100 K, the possibility of changing from excitonic to free type recombinations can be ruled out. In quantum wells, the interfacial defects [17, 18] have been demonstrated as exciton trapping centres. Typically the binding energy of such defects lies in the 2–5 meV range. These energies are comparable to our observed Stokes shifts.

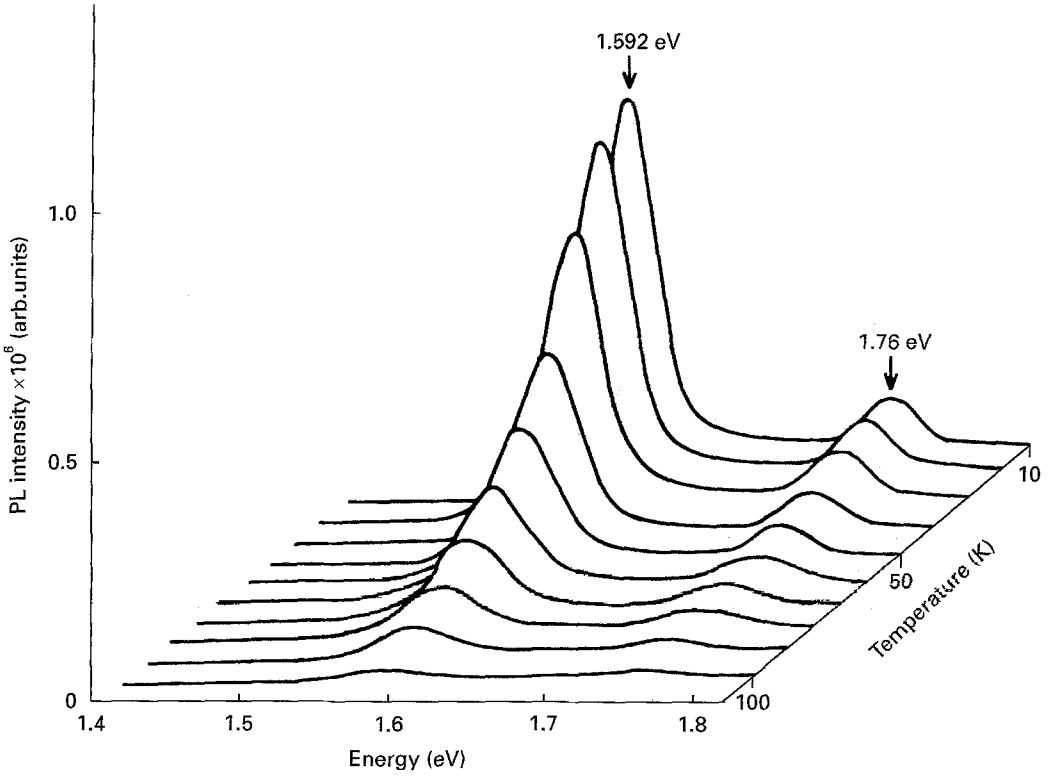

Figure 4 Photoluminescence spectra of laser structure at different temperatures, when excited, by 638 nm, normal to the layers after etching away the top GaAs layer. At 10 K, the peaks at 1.592 and 1.760 eV are from $Al_{0.08}Ga_{0.92}As$ quantum well and $Al_{0.3}Ga_{0.7}As$ barrier layers, respectively. Thickness of the quantum well is 20 nm.

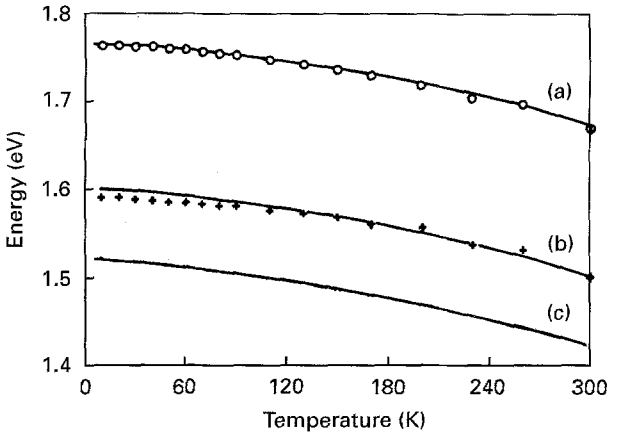

Figure 5 Transition energy versus temperature corresponding to the recombinations as observed in Fig. 3. The data points (○) and (+) represent, respectively, the recombinations associated with (a) $Al_{0.3}Ga_{0.7}As$ and (b) $Al_{0.08}Ga_{0.92}As$ QW. Solid line [curve (c)] is the band-gap variation of GaAs, which has been suitably displaced to experimental points.

Therefore, our results indicate that the excitons are bound to interfacial defects in the range 10–100 K. The recombination changes from bound exciton to free exciton above 100 K. These results are also consistent with the excitation power dependence of SQW PL intensity.

The spectral lineshape of the excitonic line in a QW can be fitted by a Gaussian curve with a broadening parameter Γ, approximately equal to the half-width at half-maximum (HWHM) of the PL peak [19]. To a first approximation, Γ can be decomposed into four different contributions: (i) interaction with acoustic phonons Γ_{LA}, (ii) interaction with LO phonons Γ_{LO}, (iii) interaction with ionized impurities Γ_I, and (iv) fluctuations of the confinement energies caused by well width variation $\Gamma_{\Delta d}$. The unresolved heavy-hole and light-hole peaks in PL contribute simultaneously to the broadening by a factor $\Gamma_{(LH-HH)}$. The free carrier density (n_s) also broadens the PL linewidth of the QW [20]. Consequently, the broadening parameter can be written as

$$\Gamma = \Gamma_{LA} + \Gamma_{LO} + \Gamma_I + \Gamma_{\Delta d} + \Gamma_{(LH-HH)} + \Gamma_{n_s} \quad (1)$$

The population of acoustic phonons goes linearly with temperature, resulting in $\Gamma_{LA} = \Gamma^0_{LA}T$. The interaction of polar optical phonon with exciton increases the linewidth as $\Gamma_{LO} = \Gamma^0_{LO}/[\exp(\hbar\omega_{LO}/kT) - 1]$, where, ω_{LO} is the optical phonon frequency. The ionized impurity scattering transition rate is proportional to the density of ionized impurity centres. Therefore, the linewidth due to ionized impurities varies as $\Gamma_I = \Gamma^0_I \exp(-\langle E_b \rangle/kT)$, $\langle E_b \rangle$ being the binding energy averaged over all impurities. Using the numerical values for GaAs, Lee *et al.* [21] have calculated the temperature dependent HWHM in meV, as

$$\Gamma^+_{tot} = (1.47 \times 10^{-3})T + \frac{4}{[\exp(\hbar\omega_{LO}/kT) - 1]} + \Gamma^+_I \exp(-\langle E_b \rangle/kT) \quad (2)$$

for the heavy-hole excitons, and

$$\Gamma^-_{tot} = (1.19 \times 10^{-3})T + \frac{2.45}{[\exp(\hbar\omega_{LO}/kT) - 1]} + \Gamma^-_I \exp(-\langle E_b \rangle/kT) \quad (3)$$

for the light-hole excitons, respectively.

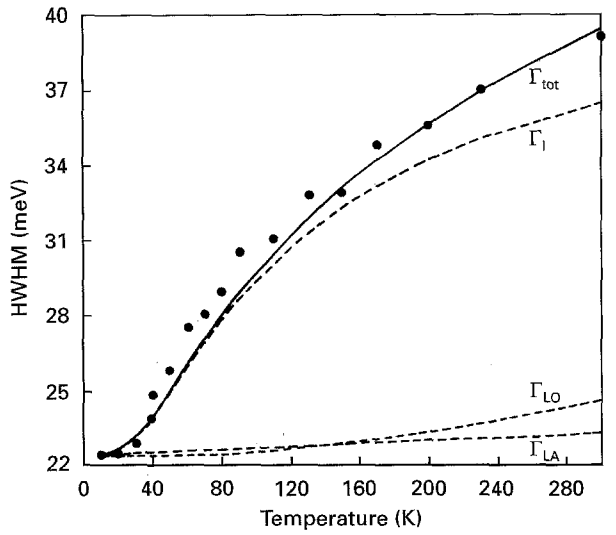

Figure 6 The half-width at half-maximum (HWHM) of the QW luminescence peak as a function of temperature. Solid circles represent the experimental points. The different (upshifted) contributions to the linewidth due to acoustical phonon scattering (Γ_{LA}), optical phonon scattering (Γ_{LO}) and ionized impurity scattering (Γ_I) are shown by dotted lines. The total HWHM is depicted by solid line.

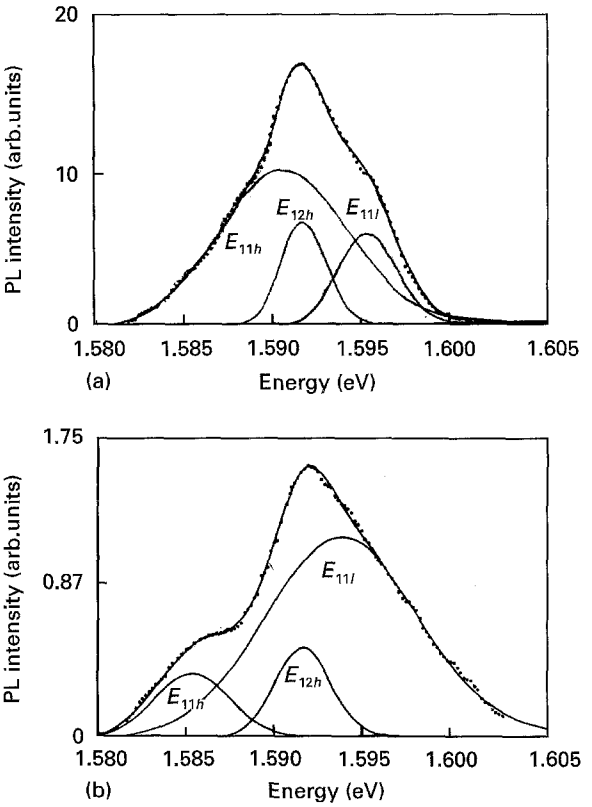

Figure 7 Luminescence spectra from $Al_{0.08}Ga_{0.92}As$ quantum well when excited by 514.5 nm light with electric field vector parallel to the layers. Curves (a) and (b) correspond to the emission polarized parallel $[Z(YY)\bar{Z}]$ and perpendicular $[Z(YX)\bar{Z}]$ to the well layers, respectively.

The observed HWHM of the QW luminescence peak as a function of temperature is shown by solid circles in Fig. 6, after giving a Gaussian fit to the experimental data. At 10 K, a HWHM of 22 meV was observed from the 20 nm $Al_{0.08}Ga_{0.92}As$ QW. The contribution of Γ_{LA}, Γ_{LO} and Γ_{n_s} to Γ at 10 K is as small as 0.3 meV [20, 21]. Therefore, it can be stated that the Γ(10 K) is a direct indication of the degree of well width fluctuation. As the temperature is raised, the QW peak broadens further, achieving a value of 37 meV at room temperature. Lee *et al.* [21]. have shown a stronger impurity ionization scattering for heavy-hole excitons compared to that for light-hole excitons. We have used $\Gamma_I^+ = 12$ meV and $\Gamma_I^- = 8$ meV, respectively, the linewidth due to ionized impurity scattering for heavy-hole and light-hole excitons and $\hbar\omega_{LO} = 36$ meV, in Equations 2 and 3, to fit the temperature variation of the observed Γ. The combined light- and heavy-hole contributions Γ_{LA}, Γ_{LO} and Γ_I are shown (22 meV upshifted) by dotted lines and the total Γ is shown by a solid line in Fig. 6 as a function of temperature. From the best fitted (± 1 meV) data, we infer the average binding energy $\langle E_b \rangle = 10$ meV for impurities in a 20 nm well. This value matches with the earlier observations [22] on temperature evolution of HWHM for light- and heavy-holes.

3.2.3. Polarization dependence

We have carefully measured the polarization dependence of SQW PL at 25 K. For this study, the sample was excited by 514.5 nm line in the geometry as shown in Fig. 1. For light propagating along the plane of layers (Z-axis), the incident electric field vector was either planar (parallel to the Y-axis) or perpendicular (parallel to the X-axis) to the plane of the well. For the planar incident electric field vector, the luminescence spectra polarized along the layers and perpendicular to the layers are shown in Fig. 7 by (a) $Z(YY)\bar{Z}$ and (b) $Z(YX)\bar{Z}$, respectively. The emission intensity was compared for in-plane ($I_\parallel$) and out-of-plane ($I_\perp$) component of PL. From these observed intensities, the average polarization ratio $\mathbf{P} = (I_\parallel - I_\perp)/(I_\parallel + I_\perp) = 0.9$ was calculated. This indicates that the luminescence is fully polarized. For the incident electric field vector perpendicular to the layers, the PL spectra polarized along the layers $[Z(XY)\bar{Z}]$ and perpendicular to the layers $[Z(XX)\bar{Z}]$ are shown in Fig. 8a and b, respectively. The average polarization ratio $\mathbf{P} = 0.5$ confirms depolarized luminescence for this excitation geometry. The PL spectra in both the excitation geometries are best fitted with three Gaussian components and the transitions are identified as E_{ijk}, where i and j are the electron and hole quantum numbers and k is the type of hole. In all the Gaussian fitted spectra, the 1.589 and 1.595 eV peaks are, respectively, the conduction electron to first heavy-hole (E_{11h}) and conduction electron to first light-hole (E_{11l}) transitions. The peak at 1.592 eV is tentatively assigned as a transition from the conduction electron to second heavy-hole (E_{12h}) emission. This parity forbidden peak is expected to gain intensity under heavy external perturbations, like electric fields, etc. The observed polarization dependent integrated intensities of E_{11h} and E_{11l} transitions for different excitation and collection geometries are summarized in Table I. These intensities of the heavy-hole and light-hole transitions in a QW can be explained, assuming a

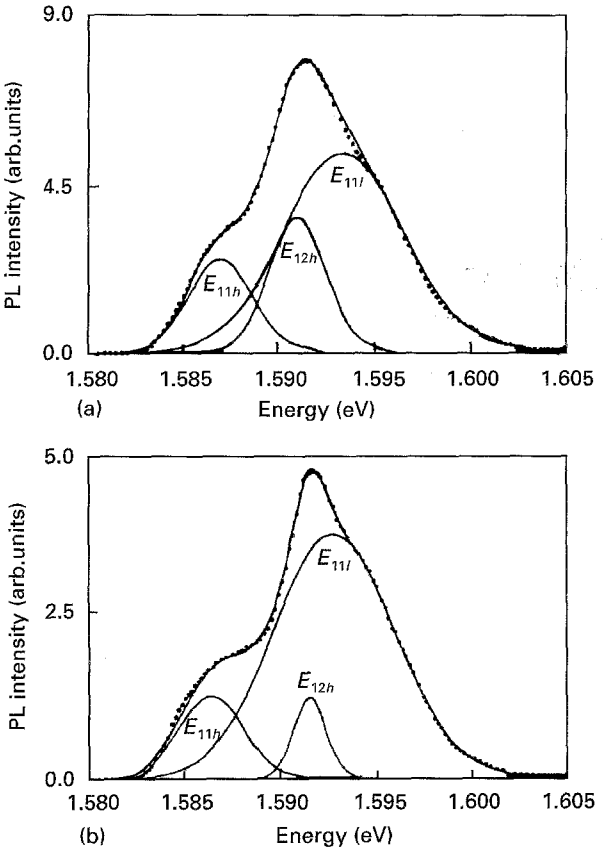

Figure 8 Luminescence spectra from $Al_{0.08}Ga_{0.92}As$ quantum well when excited by 514.5 nm light with electric field vector perpendicular to the layers. Curves (a) and (b) correspond to the emission polarized parallel $[Z(XY)\bar{Z}]$ and perpendicular $[Z(XX)\bar{Z}]$ to the layers, respectively.

TABLE I Polarization-dependent integrated intensities of heavy-hole (E_{11h}) and light-hole (F_{11l}) transitions for different excitation and collection geometries

Excitation geometry	Integrated intensity (arb. units)	
	E_{11h}	F_{11l}
$Z(YY)\,Z$	1824	488
$Z(YX)\,\bar{Z}$	4	21
$Z(XY)\,\bar{Z}$	91	366
$Z(XX)\,\bar{Z}$	25	141

small relaxation in the absorption and emission selection rules [23, 24], due to perturbations, e.g. due to valence band mixing. E_{11h} results in maximum plane-polarized and negligible cross-polarized PL intensity for an incident electric field vector parallel to the well layers. This is in good agreement with the anisotropic absorption [8] in QWs. The rotation of excitation beam polarization by 90° has resulted in a substantial decrease of in-plane E_{11h} PL intensity, which is consistent with the PLE observations [9]. The E_{11l} intensity is relatively stronger than E_{11h} intensity in this excitation geometry. Further, the selection rules forbid any heavy-hole band emission which is polarized perpendicular to the well [24]. The weak heavy-hole related cross-polarized emissions in Fig. 7b, and Fig. 8b can, therefore, be attributed to the band mixing at the ground valence sub-band.

4. Conclusion

On the basis of excitation power dependence of the luminescence peak, the strong excitonic origin of radiative recombinations in a QW is verified. Temperature dependence of QW emission shows that carrier transport is via localized states at low temperatures (below 100 K), while that at higher temperatures occurs via extended mini bands. To the best of our knowledge, we have presented for the first time, on the basis of PL studies, the polarization behaviour of heavy- and light-hole emissions. The PL was found fully polarized when the incident electric field vector was along the well layers. However the PL was depolarized for the incident electric field vector perpendicular to the well layers. Additionally, our observations of cross-polarized heavy-hole emissions suggest band mixing at the valence sub-band. We have also shown that a STM image of a cleaved quantum well in air easily quantifies the cross-sectional structure of quantum confined devices.

Acknowledgements

The authors are grateful to G. S. Thapa for technical support. This work has been supported by CSIR, India grant CSIR/Phy/9250 and NSF-EPSCoR grant EHR-9108775. HDB is grateful to CSIR for granting him the Emeritus Scientist project.

References

1. D. A. B. MILLER, D. S. CHEMLA, P. W. SMITH, A. C. GOSSARD and W. T. TSANG, *Appl. Phys.* **B28** (1982) 96.
2. T. H. WOOD, C. A. BURRUS, D. A. B. MILLER, D. S. CHEMLA, T. C. DAMEN, A. C. GOSSARD and W. WEIGMANN, *IEEE J. Quantum Electron.* **QE-21** (1985) 117.
3. D. A. B. MILLER, D. S. CHEMLA, T. C. DAMEN, A. C. GOSSARD, W. WEIGMANN, T. H. WOOD and C. A. BURRUS, *Appl. Phys. Lett.* **45** (1984) 13.
4. Y. SILBERBERG, P. W. SMITH, D. J. EILENBERGER, D. A. B. MILLER, A. C. GOSSARD and W. WEIGMANN, *Opt. Lett.* **9** (1984) 507.
5. M. YAMANISHI and I. SZEMUNE, *Jpn. J. Appl. Phys.* **23** (1984) L35.
6. Y.-C. CHANG and J. N. SCHULMAN, *Appl. Phys. Lett.* **43** (1983) 536.
7. H. IWAMURA, T. SAKU, H. KOBAYASHI and Y. HORIKOSHI, *J. Appl. Phys.* **54** (1983) 2692.
8. J. S. WEINER, D. R. CHEMLA, D. A. B. MILLER, H. A. HAUS, A. C. GOSSARD, W. WEIGMANN and C. A. BURRUS, *Appl. Phys. Lett.* **47** (1985) 664.
9. A. BALIGA and N. G. ANDERSON, *ibid.* **60** (1992) 283.
10. G. BINNING, C. GERBER, H. ROHRER and E. WEIBEL, *Phys. Rev. Lett.* **49** (1982) 57.
11. H. W. M. SALEMINK, M. B. JOHNSON and O. ALBERKTSEN, *J. Vac. Sci. Technol.* **B12** (1994) 362.
12. R. M. FEENSTRA, *Semicond. Sci. Technol.* **9** (1994) 2157.
13. J. E. FOUQUET and A. E. SEIGMAN, *Appl. Phys. Lett.* **46** (1985) 282.
14. D. S. CHEMLA, D. MILLER, P. SMITH, A. C. GOSSARD and W. WEIGMANN, *IEEE J. Quantum Electron.* **QE-20** (1984) 265.
15. E. H. BOTTCHER, K. KETTERE, D. BIMBERG, G. WEIMANN and W. SCHLAPP, *Appl. Phys. Lett.* **50** (1987) 1074.
16. R. L. GREENE and K. K. BAJAJ, *Solid State Commun.* **45** (1983) 831.
17. C. DELALANDE, M. H. MEYNADIER and M. VOOS, *Phys. Rev.* **B31** (1984) 2497.

18. J. E. ZUCKER, A. PINCZUK, D. S. CHEMLA and A. C. GOSSARD, *Phys. Rev.* **B35** (1987) 2892.
19. H. IWAMURA, H. KOBAYASHI and H. OKAMOTO, *Jpn. J. Appl. Phys.* **23** (1984) L795.
20. M. S. SKOLNICK, K. J. NASH, M. K. SAKER, S. J. BASS, P. A. CLAXTON and J. S. ROBERTS, *Appl. Phys. Lett.* **50** (1987) 1855.
21. J. LEE, E. S. KOTCLES and M. O. VASSEL, *Phys. Rev.* **B33** (1986) 5512.
22. J. LEE and M. O. VESSELL, *Jpn. J. Appl. Phys.* **23** (1984) 1086.
23. D. D. SELL, S. E. STOKOWSKI, R. DINGLE and J. V. DILRENZO, *Phys. Rev.* **B7** (1973) 4568.
24. C. WEISBUCH, in "*Physics and Applications of Quantum Wells and Superlattices*", Vol. **170** of NATO Advanced Studies Institute Series B: Physics, edited by E. E. Mendez and K. von Klitzing (Plenum Press, New York, 1987) pp. 261.

Received 9 August
and accepted 21 December 1995